Current Science
CS 5 (6), 5231-5250 (2025)
Received 14 Oct 2025 | **Accepted 28 October** 2025 | **Online Available 03 November** 2025
https://doi.org/10.52845/CS/2025-5-6-1

Current Science

Current Science

OPEN ACCESS

ISSN (O) 2795-8639

Original Article

Research on Brain-Machine Interface System Based on High-Frequency SSVEP Hand Rehabilitation Robot

Tinghang Guo[1], Xin Ji[2]*, Xiaohan Li[3], Zhuanping Qin[4] , Guangda Lu[5], Runze Li[6]

[1]Tianjin Key Laboratory of Information Sensing & Intelligent Control Automation and Electrical Engineering College, Tianjin University of Technology and Education, Tianjin, China

[2]Tianjin Key Laboratory of Information Sensing & Intelligent Control Automation and Electrical Engineering College, Tianjin University of Technology and Education, Tianjin, China

[3]Tianjin Key Laboratory of Information Sensing & Intelligent Control Automation and Electrical Engineering College, Tianjin University of Technology and Education, Tianjin, China

[4]Tianjin Key Laboratory of Information Sensing & Intelligent Control Automation and Electrical Engineering College, Tianjin University of Technology and Education, Tianjin, China

[5]Tianjin University of Technology and Education Tianjin, China;Tianjin University of Technology and Education Engineering Training Center, Tianjin 3000222

[6]Tianjin University of Technology and EducationTianjin, China

***Corresponding Author: Xin Ji**

Abstract:

Abstract: To address the limitations and poor comfort associated with traditional evoked-pattern paradigms in hand rehabilitation robots within the brain-computer interface field, a hybrid brain-computer interface system combining motor imagery (MI) and high-frequency steady-state visual evoked potentials (SSVEP) was employed. A four-category visual stimulator suitable for hand rehabilitation robots was designed. Comparative studies were conducted using different algorithms to analyze SSVEP and MI-SSVEP paradigms, collecting EEG signals from both paradigms under identical conditions. Using our self-collected dataset, we compared the proposed FB-NBPFCCA (Filter Bank Narrow Band-Pass Filtered CCA) algorithm with the Filter Bank Correlation Analysis (FBCCA) algorithm. Results indicate that the FB-NBPFCCA algorithm demonstrates superior performance in decoding action intentions under the MI-SSVEP paradigm, achieving a four-class gesture recognition accuracy of 95.5 ± 3.46% and an information transfer rate of 92.78 ± 5.65 bits/min.

Keywords brain-computer interface; high frequency; steady state visualized evoked potential; hybrid brain computer interface; hand rehabilitation

1. Introduction

Brain-computer interface (BCI) systems based on steady-state visual evoked potentials (SSVEP) have attracted much attention due to the advantages of high signal-to-noise ratio, superior information transfer rate, and good classification performance[1]. In the field of rehabilitation, SSVEP-BCI assists in the reconstruction of patients' neurological functions by converting visual stimuli into operational commands.Hochberg's team utilized implantable electrodes to enable paralyzed patients to control a robotic arm [2]; Arpaia et al. developed wearable SSVEP devices to assist in the rehabilitation of children with ADHD [3]; Jun

Xiao and Jun Qin developed a multimodal rehabilitation incorporating SSVEP respectively system and verified its effectiveness in stroke rehabilitation [4,5]. Motor imagery brain-computer interface (MI-BCI) also plays an important role in rehabilitation. kim et al. found that a rehabilitation program combining motor imagery (MI) can significantly improve the precision of upper extremity motor control in stroke patients [6]. Yunqi Ma's team confirmed that MI could enhance lower limb gait symmetry and promote functional recovery [7]. To break through the limitations of a single paradigm, the MI-SSVEP hybrid system achieves performance optimization through multimodal signal fusion.Yang's team developed a hybrid system based on 6.6-9.6Hz stimuli to achieve recognition of 10 hand movements (95.56% accuracy) [8]; Ko et al. used 15 and 20Hz visual stimuli to obtain 97.4% recognition accuracy [9]. Current studies mostly use low and medium frequency stimulation (4-30Hz), but there is a risk of inducing epilepsy and easy interference with spontaneous EEG α/β band (8-30Hz). High-frequency SSVEP not only avoids frequency overlap, but also relieves visual fatigue.Wong et al. demonstrated that high-frequency stimulation significantly reduces the user's visual fatigue index [10]; Diez's team utilized high-frequency SSVEP to achieve a stable, long-duration control of a robotic wheelchair [11]. These advances suggest that high-frequency SSVEP technology is driving the continued development of BCI in rehabilitation applications by enhancing system comfort and stability[12].

Based on this, this study designed a four-command high-frequency MI-SSVEP hybrid paradigm with a stimulation frequency range of 30-42 Hz for the clinical needs of hand function rehabilitation, collected EEG data from 20 subjects offline, and comparatively analyzed the differences in recognition performance in the high-frequency band of different SSVEP decoding algorithms to provide key technological support for the development of a robotic brain-computer interface system for hand rehabilitation that has a high control accuracy and a low fatigue characteristic. It provides key technical support for the development of hand rehabilitation robot brain-computer interface system with high control accuracy and low fatigue characteristics.

II. Methods and Experiments

A. Subjects of the Experiment

A total of 20 healthy subjects were recruited to participate in the experiment, including 18 males and 2 females, aged between 21-28 years old, all of whom had no history of neurological disease or visual impairment. Subjects were healthy, with normal or corrected-to-normal vision and no psychiatric disorders, and participation was voluntary. Prior to the start of the experiment, all subjects read the experimental procedures, potential risks and precautions, and confirmed that they fully understood the purpose of the experiment and the operational procedures, and all subjects signed a written informed consent form.

B. Experimental Design

The experiments in this study used a high-frequency SSVEP paradigm containing four independent stimulation conditions with stimulation frequencies ranging from 30 Hz to 42 Hz in 4 Hz step increments. Subjects were placed in a bright environment and sat in a comfortable position in front of a monitor at a distance of 60 cm away. The stimulus program was written by the Psychtoolbox v3.0.19 toolkit in MATLAB R2023b. Each stimulus consisted of a 360 × 360 pixel square presented on an LCD monitor of size 26 inches. The display has a high resolution of 2560 × 1440 pixels and a high refresh rate of 180 Hz to ensure clarity and stability of the visual stimuli. Based on the fact that high-frequency EEG signals are comfortable and not easy to be fatigued, a frequency of 30 Hz or more was

selected for the experiment, and the stimulation interface was shown in Fig. 1, with the four gestures of five-finger bending (30 Hz), five-finger stretching (34 Hz), thumb bending (38 Hz), and thumb stretching (42 Hz), respectively.

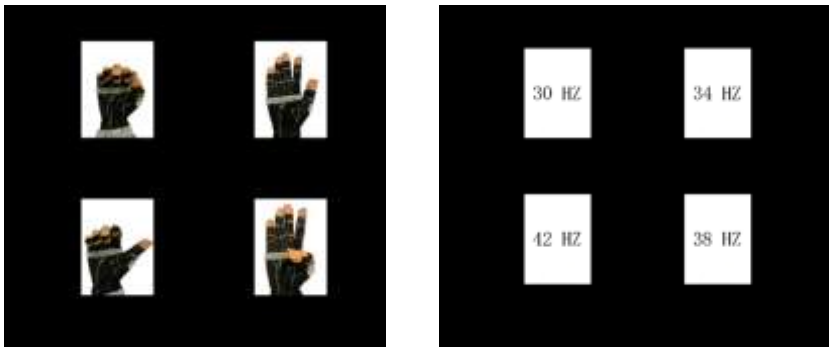

FIG. 1. Experimental interface
（a）User Interface for Hand Rehabilitation Robot Control System （b）Frequency value of the target

The experiment consisted of 4 blocks, each of which collected 40 trials of EEG data. Each block was randomly presented with 4 stimulus conditions, each repeated 10 times. Each trial lasted for 7 seconds: the first second presented a red cross in the center, and subjects were required to immediately shift their attention to the target stimulus; the target stimulus was then flashed for 5 seconds, during which they were required to avoid blinking; and after the stimulus disappeared, they rested for 1 second. To alleviate visual fatigue, a 3-minute rest period was arranged after completing each block, and the trial flow is shown in Figure 2. During the execution of the SSVEP task, a visual stimulus pattern based on the encoding of action-state blinks was used, and the stimulus was accurately presented on the screen. During the formal trial, the subject sat quietly in front of the display, with the LCD screen approximately 70 cm from the subject's eyes. The trial was started by pressing the space bar after adjusting to a calm state. The recording time for one trial was 7 seconds, and the recording time for the other trial was 7 seconds.

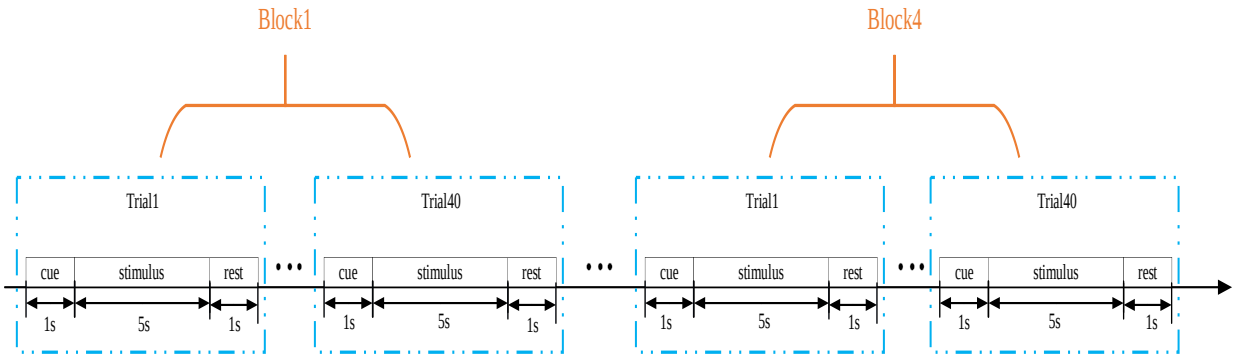

FIG. 2. Flowchart of the test

Thus, the time required to record EEG data for all stimuli was 280 seconds per session. The experiment was conducted in 4 phases, so the

minimum time required for subjects without an interval between each phase was 20 minutes.

In the MI-SSVEP experimental condition, the overall experimental flow remained consistent with the SSVEP-only condition. However, the key difference between the two was that in the MI-SSVEP condition, subjects were asked to perform a motor imagery task while focusing on the flashing visual stimuli, imagining hand movements based on the animation in the stimulus block.

A 64-lead system from Neuroscan was used for the experiment, with a sampling rate of 1000 Hz. 27 channels were selected for the experiment because the brain regions corresponding to ssvep and motor imagery are mainly occipital and parietal regions (8 leads in occipital region: PO5, PO3, POz, PO4 PO6, O1, Oz, O2; the remaining 19 leads: FC3, FC1, FCz, FC2, FC4, C3, C1, Cz, C2, C4, CP3, CP1, CP2, CP4, P5, P3, Pz, P4, P6), and the reference electrodes were located in bilateral mastoids. The impedance of all electrodes was lower than 10 kΩ, and the data were eliminated from industrial frequency interference by a 50 Hz trap, the specific electrode layout is detailed in Figure 3.

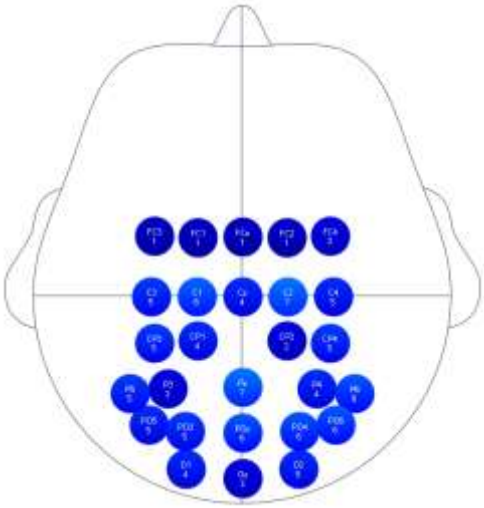

FIG. 3. Distribution of 27-lead electrode positions

III. Decoding Algorithm

A. Typical Correlation Analysis and Its Extended Algorithm

Typical correlation analysis, as an effective feature extraction method in SSVEP-BCI, improves the signal-to-noise ratio and recognition accuracy by fusing multi-channel EEG signals. Its core establishes a linear model by calculating the maximum correlation between two sets of variables to achieve accurate recognition of stimulus frequency. In the multi-target recognition task, CCA can extract the statistical correlations induced by different stimulus frequencies and provide frequency decoding strategies for the system.

The SSVEP signal consists of brain responses of the same frequency as the stimulus, harmonics (integer multiples of the fundamental) and subharmonics. In addition to the fundamental frequency components, the harmonic frequency components can also provide useful information for frequency identification. However, CCA-based frequency recognition algorithms do not make good use of the harmonic frequency components.The FBCCA algorithm is an improvement of the CCA algorithm, aiming to solve the problem that CCA ignores the

harmonic components when analyzing SSVEP signals[13,14].The FBCCA firstly decomposes the original EEG signals in subbands using N filters with different passbands, which are band-pass filters, and the decomposed sub band components are denoted as $XSBn$, where n denotes the serial number of the filter. Then, standard CCA processing is applied to each subband component separately to obtain the correlation value Yfk between the subband component and the reference signal corresponding to all stimulus frequencies, where k denotes the ordinal number of the reference signal. Finally, the correlation vector ρk is computed.

$$\rho_k = \begin{bmatrix} \rho_k^1 \\ \rho_k^2 \\ \vdots \\ \rho_k^N \end{bmatrix} = \begin{bmatrix} \rho(X_{SB_1}^T W_X(W_{SB_1} Y_{f_k}), & Y^T W_Y(X_{SB_1} Y_{f_k})) \\ \rho(X_{SB_2}^T W_X(W_{SB_2} Y_{f_k}), & Y^T W_Y(X_{SB_2} Y_{f_k})) \\ \vdots & \\ \rho(X_{SB_N}^T W_X(W_{SB_N} Y_{f_k}), & Y^T W_Y(X_{SB_N} Y_{f_k})) \end{bmatrix} \quad (1)$$

The ρ(x,y) correlation coefficient in Equation (1) represents the correlation between the variables x and y. The correlation coefficient of each subband component is multiplied by the square of the corresponding weighting factor. The square of the correlation coefficient corresponding to each subband component is multiplied by the corresponding weighting factor, and then these weighted values are summed up as the eigenvalues for target identification. The weighted sum of squares of all subband correlation coefficients Wρk is calculated as ρk.

$$W_{\rho k} = \sum_{n=1}^{N} w(n) * (\rho_k^n)^2 \quad (2)$$

In Eq. (2), n denotes the subband index. Since the signal-to-noise ratio of the SSVEP harmonic components decreases as the response frequency increases, the weighting coefficients of each subband component are defined as follows:

$$w(n) = n^{-a} + b, n \in [1, N] \quad (3)$$

In Eq. (3) n ∈ [1, N], the parameters a and b are constants, and their values are determined by the classifier performance to the best case. The values of a and b were determined by a grid search to be 1.25 and 0.25, respectively. n represents the number of sub-bands of the filter bank, and the range of values is restricted to [1:1:10], i.e., integers from 1 to 10. Ultimately, the correlation coefficient ρk corresponding to each stimulus frequency is used to identify the frequency of the SSVEP, where the frequency of the reference signal corresponding to the largest correlation coefficient is considered to be the frequency of the SSVEP.

B. Narrow Bandpass Filtered Typical Correlation Analysis

CCA is applied to the classification and identification of multilead SSVEP signals: m multichannel SSVEP signals X = (X1,X2,...Xm)T , Y is the reference signal corresponding to the stimulus frequency, CCA investigates the correlation between the two sets of variables X, Y, and finds a set of values that maximizes the correlation coefficient between

the vectors X, Y, shown in Eq. (4):

$$\max_{w_x w_y} \rho(x,y) = \frac{E\left[W_X^T X Y^T W_Y\right]}{\sqrt{E\left[W_X^T X X^T W_X\right] E\left[W_Y^T Y Y^T W_Y\right]}} \quad (4)$$

where the maximum value of ρ over Wx and Wy represents the maximum typical correlation; X is the multichannel SSVEP signal; and Y is the reference signal, which is a set of template signals constructed using sine and cosine functions at different integer multiples of frequencies. The maximum typical correlation coefficients of Wx and Wy are obtained when ρ takes the maximum value. When applying CCA to the analysis of SSVEP signals, X is generally set as a set of multichannel EEG signals, and Y is set as a set of corresponding reference signals:

$$Y = \begin{Bmatrix} \sin(2\pi\ ft) \\ \cos(2\pi\ ft) \\ \vdots \\ \sin(2\pi N_h ft) \\ \cos(2\pi N_h ft) \end{Bmatrix} \quad (5)$$

In the SSVEP signal identification process, the number of harmonics is denoted as Nh, the stimulus frequency as f, and the time as t. The identification result of the SSVEP signal can be determined by calculating the maximum typical correlation coefficient between the multichannel EEG signals and the reference signals, which corresponds to the frequency of the SSVEP signal [15,16].

Narrow bandpass filtered typical correlation analysis (NBPFCCA) is a technique that combines a narrow bandpass filter (BPF) and typical correlation analysis. This method is particularly suitable for processing signals containing specific frequency components, such as identifying frequency components in SSVEP signals The main purpose of the narrow bandpass filter is to significantly reduce the interference of background noise with the normal activity of the EEG, which in turn significantly improves the reliability of the detection accuracy.The SSVEP response consists of the fundamental frequency of the visual stimulus at different stages and its associated harmonics. The reference signal was generated using the four stimulus frequencies in the SSVEP experiment. The fundamental frequencies of the sine and cosine components were used to construct the reference data matrix:

$$Y = \left(\sin(2\pi f_m t), \cos(2\pi f_m t)\right), t = \frac{1}{S}, \frac{2}{S}, \ldots, \frac{K}{S} \quad (6)$$

where S is the sampling rate and f_m is the mth stimulus frequency. In SSVEP signal processing, NBPFCCA can effectively identify the frequency components and improve the accuracy of frequency detection by reducing background noise and artifacts. The specific algorithm structure is shown in Fig. 4.

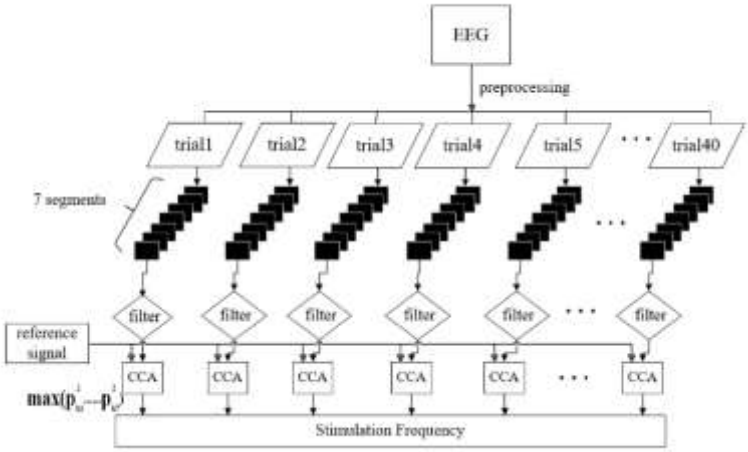

FIG. 4. Structure of the NBPFCCA algorithm

In this study, the EEG data of each subject were arranged into a 4D matrix during preprocessing, with the dimensions of "electrode channel", "time point", "target index" and "block index". "block index". When analyzing the EEG data, the EEG data were restricted to the stimulation time period of 1-5 seconds because the occipital-induced SSVEP response takes some time after the stimulation, so a limited delay needs to be taken into account. The complete EEG data was divided into 40 trials according to the markers, and each trial was divided into 7 segments by selecting a 4-second duration. A narrow bandpass filter with a bandwidth of 0.2 Hz centered on the stimulus frequency was used to filter each segment of EEG data. The correlation between the filtered data and the base frequency signal was calculated using typical correlation analysis by combining the base frequency signals at four frequencies, 30 HZ, 34 HZ, 38 HZ, and 42 HZ. The function finds the maximum value in the vector p and determines its corresponding target frequency, and the one with the largest correlation coefficient is the identified stimulus frequency. The method significantly suppresses harmonic interference and background noise through narrow-band filtering, simplifies the structure of the reference signal, and utilizes a short time window to achieve high-density frequency differentiation (0.2 Hz intervals), which is suitable for real-time brain-computer interface SSVEP signal analysis.

C. mproved Narrowband Passband Filter-Based Typical Correlation Analysis Algorithm

The NBPFCCA algorithm focuses solely on the fundamental frequency component, neglecting the harmonic information present in SSVEP signals. FBCCA decomposes the signal into multiple frequency bands, enabling separate analysis of the fundamental frequency and various harmonic components. Therefore, by leveraging the broadband information and harmonic components from FBCCA, combined with the advantage of FB-NBPFCCA in identifying specific frequencies, it achieves precise feature extraction for key frequencies. Through these enhancements, complementary advantages can be achieved, further improving the classification performance of SSVEP signals. Figure 5 illustrates the structure of the improved narrowband pass-filter typical correlation analysis algorithm:

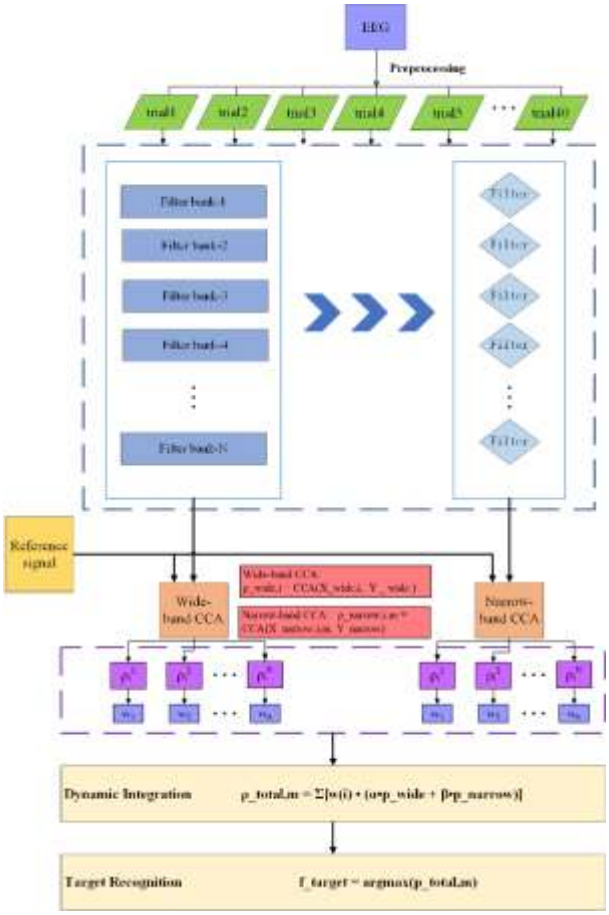

FIG. 5. FB-NBPFCCA Algorithm Structure Diagram

Based on the FBCCA filter bank architecture and incorporating the narrowband filtering concept of FB-NBPFCCA, a hierarchical filter bank structure is employed. The first layer involves wide subband partitioning using a multi-harmonic coverage partitioning method. For instance, at 30 Hz, a set of subbands is designed to cover the fundamental frequency (30 Hz) and its harmonics (60 Hz, 90 Hz, etc.). In this study, the number of subbands is set to 8, specifically: 8-16Hz, 12-24Hz, 13-32Hz, 20-40Hz, 30-50Hz, 40-60Hz, 50-70Hz, 60-88Hz. The second layer involves narrow subband partitioning, embedding 0.2Hz bandwidth narrowband pass filters within each wide subband, centered at the target stimulus frequency f_m. The narrow strap design is as follows: bandpass$(f_{\mathrm{m}} - 0.1, f_{\mathrm{m}} + 0.1)$ $\forall f_{\mathrm{m}} \in f_1, \ldots, f_N$.Performing wideband CCA on EEG data: $X_{\mathrm{wide},i} = bandpass\left(X, f_{\mathrm{low},i}, f_{\mathrm{high},i}\right)$ and Narrow-band CCA. For each wide subband $X_{\mathrm{wide},i}$ and candidate f_m: $X_{\mathrm{narrow},i,m} = bandpass\left(X_{\mathrm{wide},i}, f_m - \Delta f, f_m + \Delta f\right)$, Calculate the correlation coefficients $\rho_{\mathrm{wide},i}$ for the wide subbands $X_{\mathrm{wide},i}$ and Y_{wide} separately. Calculate the correlation coefficient $\rho_{\mathrm{narrow},i,m}$ for each narrow band $X_{\mathrm{narrow},i,m}$ and Y_{narrow}. Next, dynamic fusion is employed to compute each candidate f_m: $\rho_{\mathrm{total},m} = \sum_{i=1}^{n} \omega(i) \cdot \left(\alpha \cdot \rho_{\mathrm{wide},i} + \beta \cdot \rho_{\mathrm{narrow},i,m}\right)$, The values of α and β are dynamically adjusted based on the subband SNR. The frequency corresponding to the maximum $\rho_{\mathrm{total},m}$ is the final recognition result.

D. ERD/ERS Analysis

Event-Related Potential (ERP) is a potential change induced by an external stimulus in the cerebral cortex, which is characterized by time-locking and phase-locking. Studies have shown that both motor imagery and motor execution

can induce significant ERP components. An enhancement of the power spectra of specific EEG rhythms after stimulation is called Event-Related Synchronization (ERS); conversely, an attenuation is called Event-Related Desynchronization (ERD). The MI task in this study was related to the right hand, so C3 and its surrounding electrodes (C3, CP3, CP1, and FC3) were analyzed.

Event-Related Spectral Perturbation (ERSP) is commonly used to analyze stimulus-generated changes in the time-frequency domain.The formula for ERSP is:

$$ERSP(c,f,t)=\frac{1}{n}\sum_{g=1}^{n}|X_g(c,f,t,g)|^2 \quad (7)$$

where t is the time, c is the lead, f is the frequency value, and n is the number of trials. $X_g(c,f,t,g)$ indicates time-frequency distribution values. The ERS/ERD analysis was based on the Pfurtscheller method [17]: firstly, the EEG signal was band-pass filtered in the target frequency band; secondly, the power was calculated on a trial-by-trial basis; subsequently, the power was averaged across all trials in a superposition; and finally, the average power was calculated in a specific time window was selected as the baseline to reduce the error.

$$ERD=\frac{A-R}{R}\times 100\% \quad (8)$$

A is the average EEG power after band-pass filtering, and R is the average power of the baseline values.The ERD (Event-Related Desynchronization Score) score is used to quantify the degree of EEG power reduction in specific frequency bands by a mechanism that stems from desynchronization activity of neurons in the cerebral cortex. Lower scores indicate a higher degree of desynchronization, reflecting more widespread brain area activation.

E. Evaluation Indicators

The performance of the proposed system is evaluated using classification accuracy, information transfer rate (ITR) and SNR.ITR is an important metric to measure the performance of the SSVEP-BCI system and indicates the amount of information transferred per unit time. Another metric is classification accuracy, which refers to the rate at which the system correctly recognizes the user's intent. It is usually expressed as a percentage and the higher the accuracy rate, the greater the utility value of the system [17].The formula for ITR is as follows:

$$ITR=[\log_2 N+p\log_2 p+(1-p)\log_2\frac{1-p}{N-1}]\frac{60}{T} \quad (9)$$

Where N=4 is the number of stimulus targets to be categorized; P is the classification accuracy; T denotes the time required to execute a single command, including sight transfer time and gaze time, gaze time i.e., 5 seconds of stimulus time sight transfer time i.e., the time required to move from one gaze target to another. The signal-to-noise ratio SNR [18] is given by the formula:

$$SNR = 20\log_{10}\frac{10y(f)}{\sum_{k=1}^{5}[y(f-0.25k)+y(f+0.25k)]} \quad (10)$$

Amplitude spectra were calculated by Fast Fourier Transform , and SNR was defined as the ratio of the amplitude at the stimulus frequency to the average amplitude at 10 adjacent frequencies (i.e., 5 frequencies on each side): for each stimulus frequency, 40 experiments were first averaged to improve the SNR of the SSVEP. the average amplitude spectra were computed by averaging the amplitude spectra corresponding to the 27 channels and the 20 subjects, and then averaging the amplitude spectra was used to amplitude spectra to calculate the SNR.

A. Power Spectral Density Analysis

In this study, the spectral characteristics and signal-to-noise ratio of SSVEP are first analyzed.

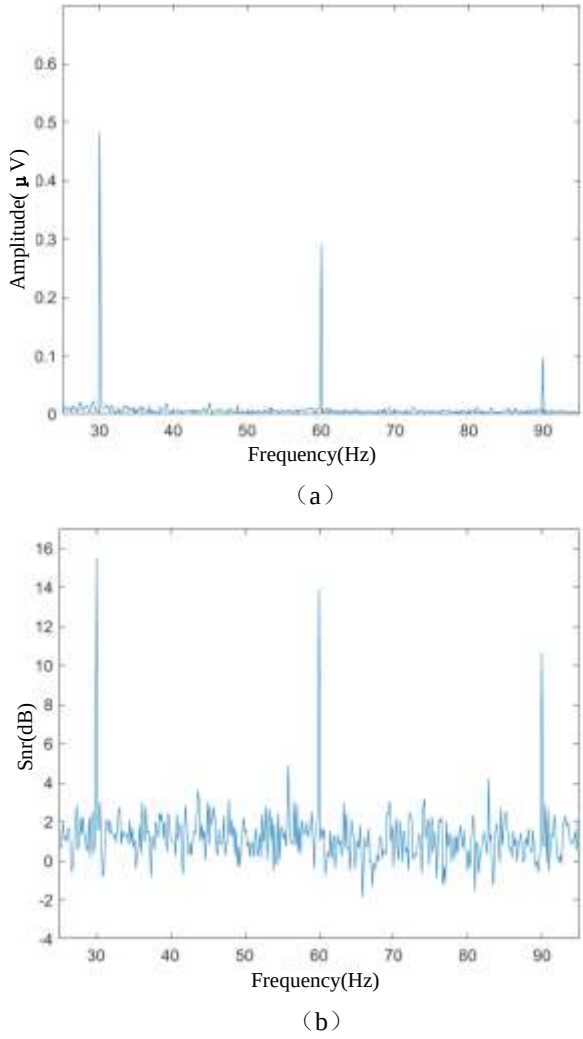

FIG. 6. 30 HZ spectrogram (a) and signal-to-noise ratio (b)

Figure 6(a) presents the average amplitude spectrum of SSVEPs at 30 Hz frequency. At this frequency, the fundamental frequency component exhibits the largest amplitude of 0.48 μV.As the frequency response increases, the amplitude of each harmonic decreases

significantly, with the first harmonic having an amplitude of 0.29 μV and the second harmonic having an amplitude of 0.09 μV.Significant peaks are present at the main frequency of 30 Hz as well as at 60 Hz and 90 Hz. The signal-to-noise ratio is measured in decibels and is calculated using the equation in Eq. 7. Fig. 5(b) demonstrates the signal-to-noise ratio of SSVEPs at 30Hz frequency. The SNR of the SSVEPs showed a slow and steady decrease as the response frequency increased (SNR of 15.49 dB for the fundamental frequency, 13.93 dB for the first harmonic SNR, and 10.66 dB for the second harmonic SNR). For all stimulus frequencies, the fundamental and second harmonics can be observed in the spectrograms, and these results show a robust and reliable frequency characterization of the fundamental and harmonic components of the SSVEP.

Iv . Experimental Results and Analysis

A. Data Model Performance Comparison

In order to evaluate the performance of different methods, the FBCCA and FB-NBPFCCA algorithms were used to process the same dataset in this experiment.The classification accuracy and ITR were calculated to compare the results of different algorithms. In order to evaluate the effect of the introduction of MI task on the system accuracy, the average accuracy and ITR for different window lengths under SSVEP and MI-SSVEP conditions were calculated, as shown in Fig. 7.

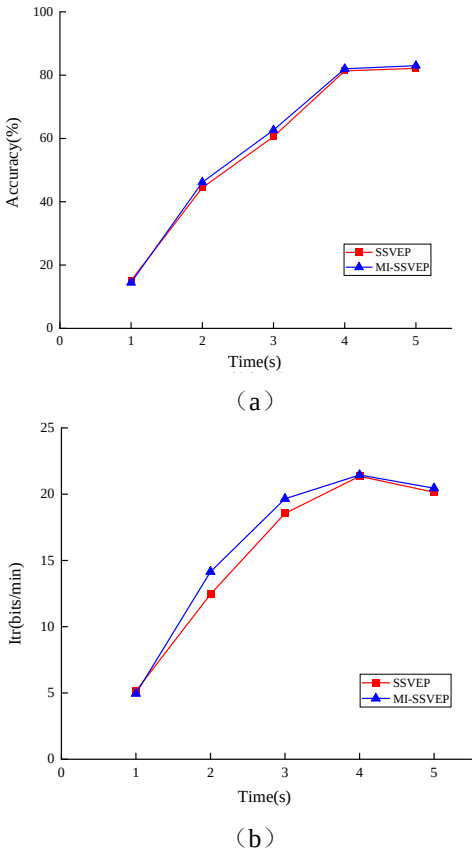

FIG. 7. Average accuracy (a) and ITR (b) for different data lengths

Figure 7(a) shows the relationship between data length and classification accuracy, where the average accuracy of both paradigms increased as the window length was lengthened. the average accuracies for the 4-second window were 81.35

± 2.15% and 82.05 ± 2.05%, respectively. The results indicate that the addition of the motor imagery task did not lead to a decrease in SSVEP recognition accuracy. Figure 6(b) shows the average ITR for different data lengths, and the average ITR showed a trend of increasing and then decreasing, with an increase in ITR in the MI-SSVEP condition relative to SSVEP at time window lengths of 2 to 3 seconds. At time window length of 4 seconds, ITR peaked for both SSVEP and MI-SSVEP conditions.

The accuracy rates of SSVEP and MI-SSVEP were calculated for 20 subjects under 4-second data conditions. Figure 8 shows the recognition accuracy rates for subjects with 4-second data using the FBCCA algorithm, NBPFCCA algorithm, and FB-NBPFCCA algorithm under different paradigm conditions.

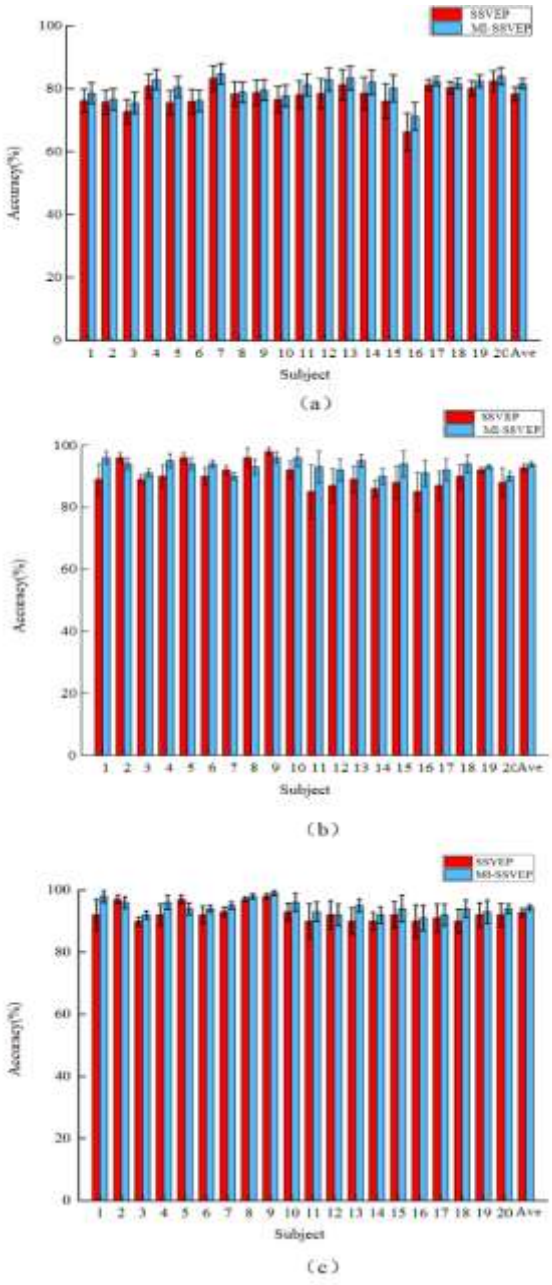

FIG. 8. Comparison of subject recognition accuracy
(a) FBCCA algorithm (b) NBPFCCA algorithm (c) FB-NBPFCCA algorithm

Figure 7(a) shows the accuracy rates calculated by the FBCCA algorithm for 20 subjects under

SSVEP and MI-SSVEP conditions. Under the SSVEP experimental condition, the average classification accuracy was 78%, while under the MI-SSVEP experimental condition, the average classification accuracy was 81%. Figure 7(b) shows the accuracy rates of the NBPFCCA algorithm under different experimental conditions. Under the SSVEP experimental condition, the average classification accuracy reached 92.8%, while under the MI-SSVEP experimental condition, the average classification accuracy was 93.9%. Figure 7(c) shows the accuracy of the FB-NBPFCCA algorithm under different experimental conditions. Compared to the previous two algorithms, this algorithm demonstrated improved overall recognition accuracy under both experimental conditions. Subjects 8 and 9 achieved recognition accuracies of 98%, while multiple subjects achieved accuracies exceeding 95%. The proposed algorithm exhibited more pronounced improvements under the mixed paradigm condition. To investigate whether there exists a statistically significant difference in classification accuracy between the SSVEP and MI-SSVEP experimental conditions, a paired t-test was employed to conduct rigorous statistical analysis of classification accuracy within each group. The results indicated that the difference in classification accuracy between the two conditions was not statistically significant ($p=0.2$). This suggests that the concurrent execution of the motor imagery task did not significantly affect the recognition accuracy of SSVEP signals. Under both SSVEP and MI-SSVEP conditions, the participants' attentional focus during the SSVEP task was comparable.

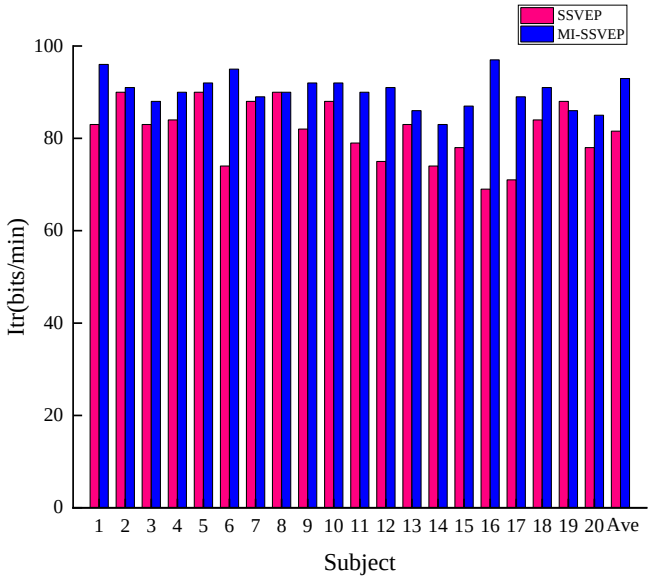

FIG. 9. Comparison of information transfer rate of the subjects

Figure 9 shows the ITR performance of the FB-NBPFCCA model for both SSVEP and MI-SSVEP paradigms in 20 subjects, showing the dual characteristics of group convergence and individual divergence: the overall average ITR was around 85 bits/min, indicating that the two paradigms had similar information transfer efficiency at the group level, however, there were significant differences at the individual level, for example, the ITRs of subjects 1, 6, and 16 under the MI -SSVEP paradigm had an ITR of about 95 bits/, a 10% improvement over SSVEP, while the SSVEP of subject 19 countered MI-SSVEP by about 2%, revealing the differential impact of differences in excitability

of the visual cortex and multimodal neural coupling effects on the performance.MI-SSVEP improves the interference resistance through multichannel acquisition; the group of neurological remodeling is more suitable for the MI-SSVEP stimulation protocol. Of the two paradigms, the MI-SSVEP paradigm has better information transfer capabilities. A system with a high ITR value means that the user is able to communicate or control the hand rehabilitation robot faster through the brain-computer interface.

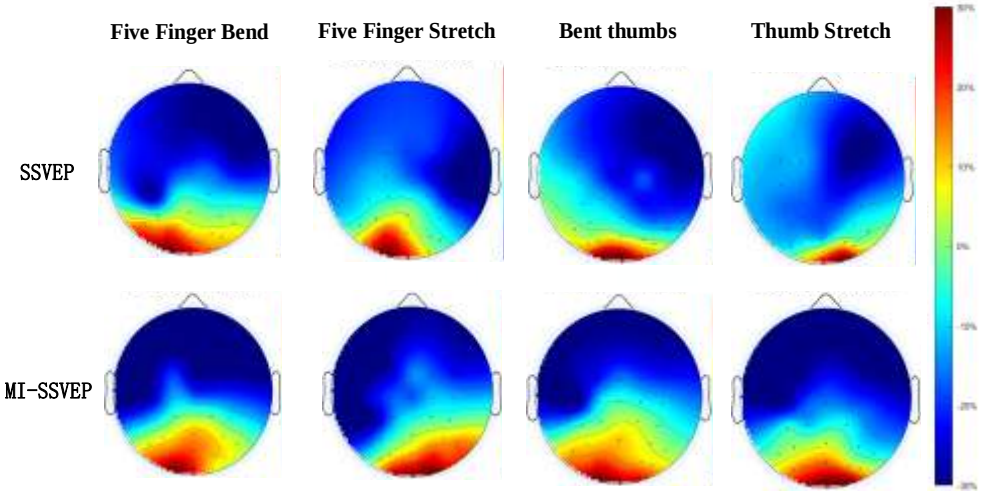

FIG. 10. EEG topography of four gestures

Figure 10 shows the EEG topography of the four gestures in the SSVEP and MI-SSVEP conditions, which visualizes the physiological characteristics of the two types of neural signals and their spatial distributions in the hybrid BCI system.The MI and SSVEP signals are spatially concentrated in the sensory-motor cortex and visual cortex, respectively, and the characteristics of the two do not interfere with each other. All gestural tasks evoked elevated energy in occipital areas, indicating that visual stimuli evoked steady-state visual evoked potentials in the occipital cortex, showing the strength of SSVEP responses in occipital areas. When imagining stretching movements, the activation level of the motor cortex was higher during five-finger stretching than during thumb stretching. The EEG energy differences under different tasks indicated that the subjects effectively performed the four different gesture MI tasks.

Analysis of the confusion matrices can determine whether there is a systematic bias in the categorization error patterns of the four gesture categories, as well as visualize the degree of inter-category confusion. The confusion matrix was computed to compare the recognition performance between categories, as shown in Figure 10.

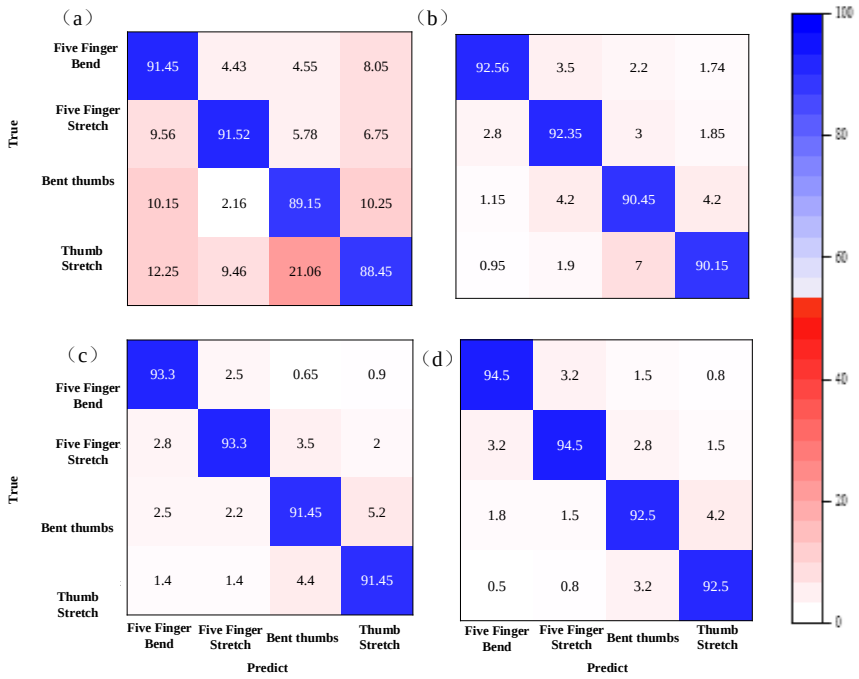

FIG. 11. Confusion matrix for recognition accuracy
(a) FBCCA algorithm SSVEP task (b) FBCCA algorithm MI-SSVEP task (c) FB-NBPFCCA algorithm SSVEP task (d) FB-NBPFCCA algorithm MI-SSVEP task

Figure 11 demonstrates the confusion matrix of the recognition accuracy for different task cases, with the diagonal lines indicating the accuracy of correct classification, as shown in Fig. 11(a) and (b), the accuracy of correct recognition in the SSVEP and MI-SSVEP tasks is around 80% when the FBCCA algorithm is employed. As shown in Fig. 11(c) and (d),the correct recognition accuracy in both task situations reached 90% and above when using the FB-NBPFCCA algorithm, with the highest performance of 94.5% in the MI-SSVEP task, indicating that the subject population responded stably to the visual stimuli. The results demonstrate the robustness and generalizability advantages of the FB-NBPFCCA algorithm in the MI-SSVEP task.

B. ERD Characterization

Effective performance of the MI task is essential to promote neurological recovery in patients, thus assessing MI performance under different conditions. Figure 12 demonstrates the subjects' ERD scores calculated in the alpha and beta bands of the C3 channel during the task. The results show that the weakest ERDs were presented during the SSVEP-only task, suggesting limited motor cortex desynchronization effects triggered by visual observation. Compared to the SSVEP alone condition, performing both MI and SSVEP tasks resulted in significantly enhanced ERDs ($p=0.006<0.01$), reflecting that the introduction of the MI task significantly elevated neural engagement. However, the ERD levels induced by the MI-SSVEP paradigm were still lower than those observed when the MI task was performed alone, and this discrepancy may be due to the parallel processing of the SSVEP task distracting the subjects' attention from the MI.The ERD scores confirmed that the designed system has good neural coupling and potential clinical applications.

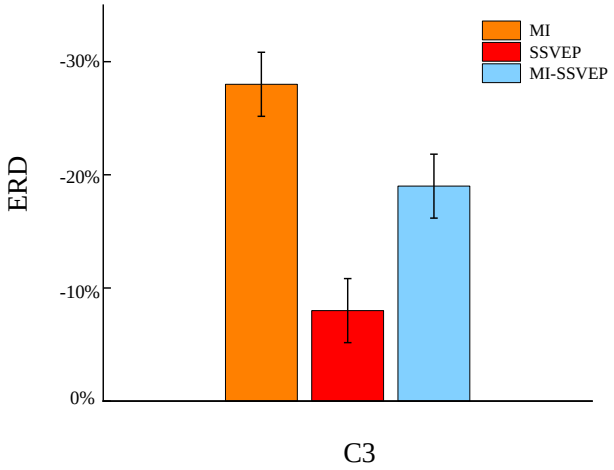

Fig. 12. ERD scores of C3 channels in α and β bands in different paradigms

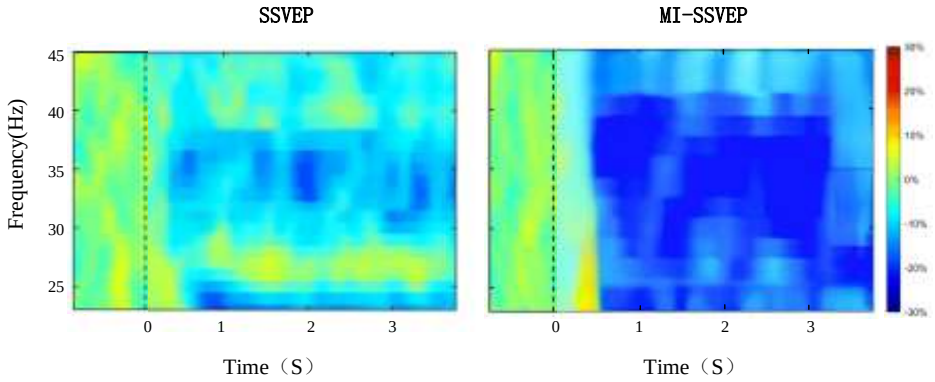

Fig. 13. Average ERSP for C3 channel

To further analyze the ERD phenomenon, the average event-related spectral perturbation (ERSP) of the C3 channel data was calculated for all subjects in different task conditions as in Figure 13. Overall, the results were consistent with the previous findings: the MI-SSVEP task induced a more significant ERD phenomenon compared to the single SSVEP task.

V. Discussion

In the field of hand function rehabilitation after stroke, traditional rehabilitation training systems generally face the problem of limited neuromodulation efficiency. In this study, the MI-SSVEP hybrid brain-computer interface paradigm is combined with the FB-NBPFCCA algorithm to construct a technological framework that is both biocompatible and practical for engineering for hand rehabilitation robotic systems through the synergistic and synergistic effects of the bimodal neural features, which enhances the control accuracy while maintaining the level of neuroplasticity. The unique advantages of this innovative technology combination are reflected in three dimensions: the MI paradigm activates the neural circuits in the motor cortex through motor imagery training, and the SSVEP paradigm maintains the state of attention through high-frequency visual stimulation, and the dynamic coupling of the two in the temporal dimension creates a closed-loop neural remodeling mechanism of "active training-immediate feedback"; at the signal processing level, the FB-NBPFCCA algorithm effectively solves the neural plasticity problem through the introduction of a narrowband filtering

mechanism. At the signal processing level, the NBPFCCA algorithm effectively solves the feature extraction problem of high-frequency SSVEP signals under nonlinear interference by introducing a narrow-band filtering mechanism; at the system application level, the motion state coding design of the four-classification visual stimulator transforms the discrete commands of traditional SSVEP-BCI into continuous motion control, which significantly improves the naturalness and functionality of rehabilitation training.

Aiming at the problem that high-frequency SSVEP signals are susceptible to myoelectric artifacts and background α-wave interference, the FB-NBPFCCA algorithm employs a narrow bandpass filter with a bandwidth of 0.2 Hz for signal processing, which eliminates the harmonics in the EEG signals and suppresses out-of-band noise effectively. The experimental results show that the average recognition accuracy of the FB-NBPFCCA algorithm reaches 95.5±3.46% in the frequency band of 30-42Hz, which is 7.2 percentage points higher than that of the traditional FBCCA method, and the information transfer rate is enhanced to 92.78±5.65bits/min, which significantly strengthens the classification performance of the model.

The clinical value of this system is reflected in the construction of a closed-loop regulatory mechanism for neurorehabilitation. Compared to the invasive motor cortex electrode system developed by Hochberg's team, this system achieves a similar level of motor control accuracy (92.25%) through non-invasive technology, while avoiding the clinical risk of implantation surgery. Compared with the single-channel SSVEP-BCI system of the Arpaia team, the multichannel data can provide more comprehensive spatial information and enhance the classification accuracy of SSVEP-BCI.

In terms of neuroplasticity, there is ample evidence that the system can effectively promote neural remodeling. While maintaining high-precision control, the system continuously activates motor-related neural networks through the MI task, which can activate motor-sensory multi-brain area networks and enhance neuroplasticity compared with the SSVEP task alone. In a study by the Institute of Automation of the Chinese Academy of Sciences, in collaboration with the Macau University of Science and Technology and the Beijing Boai Hospital team [19], an adaptive hybrid brain-computer interface rehabilitation training based on MI-SSVEP was conducted on stroke patients for 8 weeks, and it was found that the gray matter density of the motor cortex of the patients had increased by an average of 8.3%, and the strength of the functional connectivity of the motor-related brain regions had been significantly enhanced by the fMRI test, which directly demonstrates the positive impact of the system on neuroplasticity. In terms of rehabilitation value, this system can significantly improve the hand function of patients. In the clinical experiment, 10 patients with hand dysfunction after stroke were selected and randomly divided into the experimental group and the control group, with 5 cases in each group. The experimental group used this system to carry out rehabilitation training, and the control group used traditional rehabilitation training methods with a training cycle of 12 weeks. After the training, the Fugl-Meyer Assessment Scale (FMA) was used to assess the hand function of the patients, and the FMA score of the patients in the experimental group improved by an average of 18.6 points, and the average of the control group improved by an average of 9.2 points, and the experimental group's degree of improvement was significantly better than that of the control group. At the same time, the ability of patients in the experimental group to perform activities of daily living (e.g., dressing, eating, etc.) was also significantly improved, and the quality of life scores

improved by an average of 23.5 points.

In this study, at the signal acquisition level, the application of high-frequency SSVEP stimulation significantly reduces visual fatigue, allowing the duration of a single training session to be extended to more than 45 minutes; the motor-sensory closed-loop feedback generated by real-time brain-computer interaction promotes the functional reorganization of damaged neural networks and the remodeling of the corticospinal tract. Compared with the multimodal BCI system of Xiao Jun's team, the optimized processing of high-frequency SSVEP signals by the NBPFCCA algorithm extends the applicable frequency band of the system to more than 30 Hz. In addition, the high-frequency SSVEP stimulation characteristics make it suitable for patients with photosensitive epilepsy risk. Won's team's study confirms that visual stimulation above 30 Hz can reduce the incidence of photosensitive reaction to less than 0.3%, which greatly expands the scope of the system's applicability to the patient population.

Stimuli in the thumb-extension state in the confusion matrix plot are recognized as thumb-bending stimuli. This result is attributed to the overlap between the thumb extension and flexion animation movements, leading to greater ease of confusion.The lack of activation of the MI task-dependent sensorimotor cortex indirectly affects the allocation of attention in the SSVEP. The low misclassification rates for the other gestures indicate that subjects had consistent recognition results across experimental conditions, did not significantly decrease due to increased task complexity (introduction of motor imagery), and were able to effectively discriminate between the EEG features of the different gestures. Low gesture misidentification rate is the core guarantee for the hand rehabilitation robot to realize accurate rehabilitation intervention. For stroke patients, a low misjudgment rate means that the hand rehabilitation robot can recognize the patient's motor intention (e.g., finger grasping) with high accuracy and provide matching assistive force or visual feedback in real time, thus ensuring the motor accuracy of the rehabilitation training and the effectiveness of the neuroplasticity stimulation.

VI. Conclusion

(1) A brain-computer interface (BCI) rehabilitation system based on a hybrid MI-SSVEP paradigm was constructed to provide visual guidance of motor imagery synchronized with the evoked high-frequency SSVEP response through a dynamic flicker encoding mechanism, in which recognition accuracy, as a core index for the system to effectively capture the user's motor intention and visual stimulus response, directly guarantees the reliability of command recognition. For neural mechanisms that do not differ significantly from SSVEP alone, this hybrid paradigm is valuable for a hand rehabilitation robotic BCI system that fuses active motor intention recognition with external visual stimulus response. It provides a key method for realizing more natural neurorehabilitation interventions.

(2) The proposed FB-NBPFCCA algorithm demonstrates optimal classification performance in MI-SSVEP tasks, providing critical technical support for developing high-frequency SSVEP-BCI systems. It holds significant application value for building more comfortable and user-friendly SSVEP-BCI systems.

Declarations

Ethics Approval and Consent to Participate

The experiment was approved by the Ethics Committee of Tianjin University of Technology and Education.

Consent for Publication

All authors have read and agreed to the published version of the manuscript.

Availability of Data and Material

The data analyzed in this study can be obtained by contacting the corresponding author.

Competing Interests

The authors declare no conflict of interest.

Funding This research received no external

funding.

Authors' Contributions

Conceptualization, Tinghang Guo. and Xin Ji; methodology, Xiaohan Li; software, Zhuanping Qin; validation, Tinghang Guo., Xin Ji. and Xiaohan Li.; formal analysis, Zhuanping Qin.; investigation, Tinghang Guo.; resources, Xin Ji.; data curation, Xiaohan Li.; writing—original draft preparation, Xin Ji.; writing—review and editing, inghang Guo.; visualization, Tinghang Guo; supervision, Xin Ji.; project administration, Xiaohan Li.

Acknowledgments

Research Program Project of Tianjin Municipal Education Commission (2021KJ011);
Jinnan District's "Unveiling the List of Commander-in-Chief" Science and Technology Program Project (2023JB02)

Reference

1. SUN Q,CHEN M,ZHANG L,et al.Improving SSVEP Identification Accuracy Via Generalized Canonical Correlation Analysis [C] // 2021 10th International IEEE/EMBS Conference on Neural Engineering (NER), 2021:61-64.
2. Hochberg L R, Daniel B, Beata J, et al. Reach and grasp by people with tetraplegia using a neurally controlled robotic arm [J]. Nature, 2012, 485(7398): 372-375.
3. Arpaia P, Duraccio L, Moccaldi N, et al. Wearable brain-computer interface instrumentation for robot-based rehabilitation by augmented reality[J]. IEEE Transactions on Instrumentation and Measurement, 2020, 69(9): 6362-6371.
4. Jun Xiao. Research on brain-computer interface technology for clinical referencing [D]. Guangzhou: South China University of Technology, 2018(in Chinese).
5. Qin Zhun. Research on wearable brain-computer interface system for stroke rehabilitation [D]. Shanghai: Shanghai Jiao Tong University, 2020(in Chinese).
6. KOHO P,AHO S,KAUTIAINEN H,et al.Test -retest reliability and comparability of paper and computer questionnaires for the Finnish version of the Tampa Scale of Kinesiophobia [J] . Physiotherapy ,2014,100 (4):356-362.
7. Ma Yunqi, Song Zhiliang. Research on the efficacy of motor imagery therapy combined with weight-loss walking training on the rehabilitation of lower limb motor function in stroke patients [J]. Neijiang Science and Technology, 2023, 44(9):35-37(in Chinese).
8. Y.J.Yang, E.J.Jeon, J.S. Kim, and C. K.Chung,"Characterization of kinesthetic motor imagery compared with visual motor imageries," Sci.Rep., vol. 11, no. 1,p. 3751, Feb. 2021.
9. L.-W. Ko, O. Komarov, and S.-C. Lin, "Enhancing the hybrid BCI performance with the common frequency pattern in dual-channel EEG,"IEEE Trans. Neural Syst. Rehabil. Eng., vol. 27, no. 7, pp. 1360–1369, Jul. 2019.
10. Wong C M, Wang B, Wang Z, et al. Spatial filtering in SSVEP-based BCIs: Unified framework and new improvements[J], 2020, 67(11): 3057-3072.
11. Diez P F, Mut V A, Avila Perona E M, et al. Asynchronous BCI control using high-frequency SSVEP[J]. Journal of Neuroengineering and Rehabilitation, 2011, 8(1): 1-9.
12. NGUYEN T-H, CHUNG W-Y. A single-channel SSVEP-based BCI speller using deep learning[J]. IEEE Access, 2018, 7: 1752-1763.
13. Amareswar E, Naik M R, Prasad S, et al. Design of Brain Controlled Robotic Car using Raspberry Pi[C]. 2021 5th International Conference on Trends in Electronics and Informatics (ICOEI), 2022: 185-189.
14. Chen X, Zhao B, Wang Y, et al. Control of a 7-DOF robotic arm system with an SSVEP-based BCI[J]. International journal of neural systems, 2020, 28(08): 18-33.
15. Middendorf M,McMillan G,Calhoun G,Jones K S. Brain-computer interfaces based on the steady-state visual-evoked response. J]. IEEE transactions on rehabilitation engineering : a publication of the IEEE Engineering in Medicine and Biology Society,2022,8(2).
16. J. Su et al. An Adaptive Hybrid Brain–Computer Interface for Hand Function Rehabilitation of Stroke Patients [J].IEEE Transactions on Neural Systems and

Rehabilitation Engineering, 2024（32）:2950-2960.
17. Liu Q, Chen K, Ai Q, et al. Review: recent development of signal processing algorithms for SSVEP-based brain computer interfaces [J]. Journal of Medical & Biological Engineering, 2014, 34(4): 299-309.
18. Deep Soni, Nitesh Singh Malan, Shiru Sharma. CCA Model with Training Approach to Improve Recognition Rate of SSVEP in Real Time[C].Proceedings of 2019 3rd International Conference on Artificial Intelligence and Virtual Reality (AIVR 2019).,2019:47-50.
19. GAO Z,DANG W,LIU M,et al.Classification of EEG signals on VEP-based BCI systems with broad learning[J].IEEE Transactions on Systems,Man,and Cybernetics: Systems, 2020,51(11):7143-7151